www.czasopisma.pan.pl PAN POLSKA AKADEMIA NAUK www.journals.pan.pl

Arch. Metall. Mater. **69** (2024), 1, 87-90

DOI: https://doi.org/10.24425/amm.2024.147791

JEONGHA LEE[1], KUN-JAE LEE[1*]

THE EFFECTS OF THE POLYMERS AS A SACRIFICED MATERIAL FOR THE HYDROXYAPATITE POWDER SYNTHESIZED BY AN ULTRASONIC SPRAY PYROLYSIS PROCESS

The HAp (hydroxyapatite) excellent ion exchange resin and has adsorption properties of heavy metals and organic materials. It is used as an adsorption material and as an organic drug-delivery material due to these characteristics, that are essentially controlled the specific surface area. In this paper, the specific surface area was controlled by adding polymers of polyvinylpyrrolidone (PVP), polystyrene beads (PSB), and polyethylene glycol (PEG). Through the USP process, the HAp powder is able to synthesize into the spherical shape, specific surface area, and pore were controlled by the properties of the polymers.

Keywords: Hydroxyapatite; Ultrasonic Spray Pyrolysis; powder; specific surface area

1. Introduction

Hydroxyapatite ($Ca_{10}(PO_4)_6(OH)_2$; HAp) is the inorganic compound based on the calcium phosphate, which has a composition and structure similar to human bones [1-3]. Thus, it is being used in the various fields such as the implants and the bone supports [4-5]. In addition, the HAp is used in the environmental fields including the adsorption of the heavy metals and organic substances, air purification filters, and adsorbents, due to the characteristics such as the high removal ability and organic matter adsorption against divalent heavy metal ions [6-9]. The adsorption performance essentially improves the specific surface area through a surface modification. Moreover, it is necessary to control the morphology of the particles [10].

The surface modification generally is conducted the additional process after the powder synthesized process. In contrast, in the USP process, by adding a polymer material to the precursor solution, it is possible to have a surface modification effect simultaneously with powder synthesis [11-12]. In the USP process, the precursor solution passes through the reactor in the form of droplets due to the ultrasonic atomizing and carrier gas injection. The solvent is evaporated, and particles are synthesized through thermal decomposition [13]. At this time, the synthesized particle properties were controlled by adjusting process parameters at low cost, and porous structures using polymers during the USP process were also studied [12,14-16].

In this study, it aimed to control the specific surface area by synthesizing spherical HAp during the USP process with the polymer addition as the sacrificed materials. The polymers used for the specific surface area control were polyvinylpyrrolidone (PVP), polystyrene beads (PSB), and polyethylene glycol (PEG). The difference in the morphology and specific surface area of the powder synthesized by adding hydrophilic PVP and PEG was investigated [17-18]. Also, hydrophobic PSB was compared with hydrophilic PVP and PEG to clarify the mechanism [19].

2. Experimental

The calcium nitrate tetrahydrate (ALDRICH, 99.0%) and phosphoric acid (DAEJUNG, 85%) were used as the precursors to synthesis of the HAp. The precursor solution was prepared by fixing to 1 M (Ca/P = 1.67) in D.I water as a solvent.

To treat the surface of the HAp powder, polyvinylpyrrolidone ($(C_6H_9NO)_n$, ALDRICH, Mw = 55,000 g/mol), polyethylene glycol ($H(CH_2CH_2O)_nOH$, DAEJUNG, Mw = 400 g/mol), and synthesized polystyrene beads ($(C_8H_8)_n$, beads size: 163 nm ± 16 nm) was used as the sacrificial materials to increase of the specific area. They were used in the above solution according to the volume ratio of HAp : Polymer = 1 : 1, followed by stirring at room temperature [20]. In the USP process, the temperature of the reactor composed of the two heating units

[1] DANKOOK UNIVERSITY, DEPARTMENT OF ENERGY ENGINEERING, CHEONAN 31116, REPUBLIC OF KOREA

[*] Corresponding author: kjlee@dankook.ac.kr

was fixed to the first heating unit 200°C and the second heating unit 800°C. The air was used as the carrier gas, the flow rate was fixed at 3 L/min, and the prepared solution injection rate was fixed at 0.4 mL/min. The USPed powder was conducted collected in a collector. The prepared powder was additional heat treatment at 600°C for 2 h. This process was performed to remove residual polymer and the dense structure.

The X-ray diffraction (XRD, ULTIMA IV, Rigaku) was analyzed to confirm the phase of the produced powder. The crystallite size of the powder was calculated by Debye Scherrer equation: $D_{hkl} = K\lambda(B_{hkl}\cos\theta)$, where D_{hkl} is the crystallite size in the direction perpendicular to the lattice planes, hkl are the Miller indices of the planes being analyzed, K is a numerical factor frequently referred to as the crystallite-shape factor, λ is the wavelength of the X-ray, B_{hkl} is the width (FWHM) of the X-ray diffraction peak in radians and θ is the Bragg angle [21]. The morphology and particle size were observed using the Field Emission Scanning Electron Microscopy (FE-SEM, SIGMA 500, CARL ZEISS). The specific surface area of the HAp powder was analyzed by the Brunauer-Emmett-Teller (BET, 3Flex Version 4.05 MICROMERITICS).

3. Results and discussion

Fig. 1(a) shows the phase of the raw USPed powder and additional heat-treated powder by the XRD analysis, that they were confirmed to the HAp phase. The crystallite sizes calculated from the FWHM values were 18 nm and 23 nm of the raw USPed HAp powder and additional heat-treated HAp powder, respectively. Fig. 1(b)-(c) show the SEM images of the raw USPed HAp powder and additional heat-treated HAp powder that were observed in the spherical shape. The additional heat-treated HAp powder surface was rougher than that of the raw USPed HAp powder. The difference of the HAp powder surface roughness was suggested that the additional heat treatment increases the crystallite size of the HAp.

The XRD patterns show the phase analysis results of the USPed powder synthesized by adding polymer (Fig. 2(a)) and the additional heat-treated powder (Fig. 2(b)). According to the phase analysis results of the USPed powder prepared by adding the polymer and the additional heat treatment powder, it was found that they were synthesized in the same HAp phase regardless of the type of polymer. Therefore, it was possible

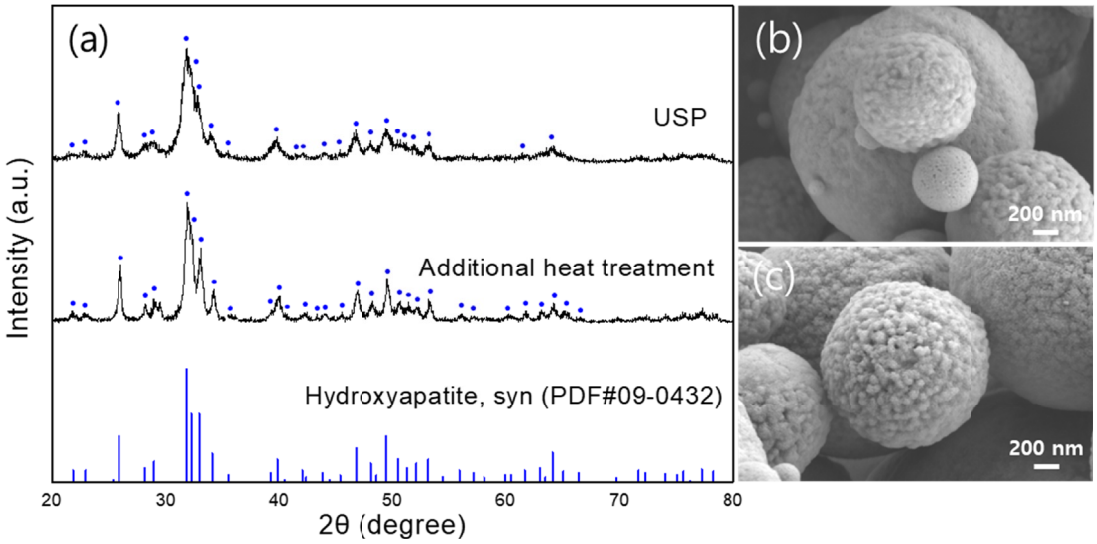

Fig. 1. (a) XRD analysis results of the raw HAp synthesized via USP process and additional heat treatment at 600°C for 2 h, FE-SEM results of raw HAp synthesis via (b) USP process and (c) additional heat treatment at 600°C for 2 h

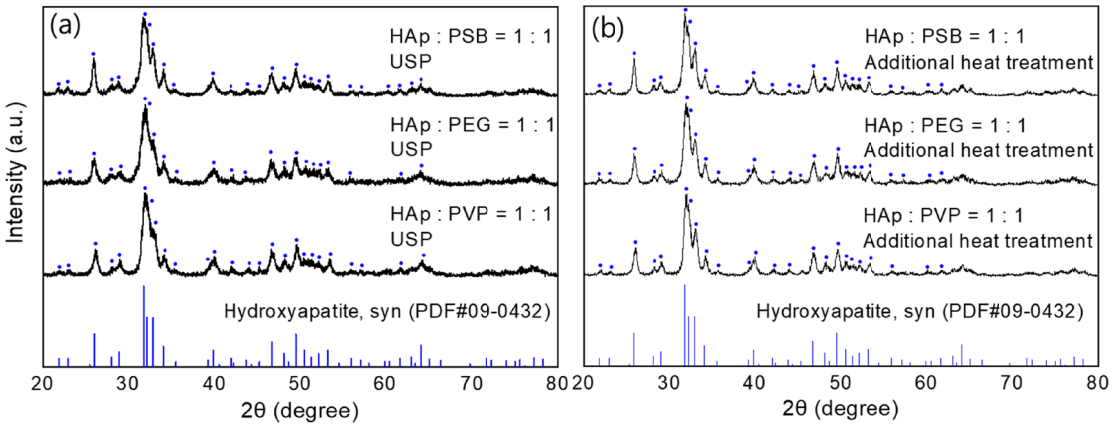

Fig. 2. XRD patterns of the prepared powder adding polymers as (a) USP process and (b) additional heat treatment at 600°C for 2 h

to control the specific surface area of the pure HAp powder without phase change and the appearance of a second phase by adding a polymer. For the USPed HAp powder prepared by adding each PVP, PSB, and PEG polymer, the crystallite size by the FWHM of XRD results was calculated to be 15 nm, 18 nm, and 14 nm, and for the additionally heat-treated HAp powder, it was 17 nm and 19 nm and 16 nm, respectively. As a result of FWHM synthesis of HAp by addition of polymer, the crystal size of USPed HAp powder and HAp powder subjected to additional heat treatment was similar. Through this, it was considered that the polymer inhibited the growth of HAp particles during the particle synthesis process [22].

The shape of the both USPed (Fig. 3(a)-(c)) and additional heat-treated HAp powders (Fig. 3(d)-(f)) with the polymer addition and were observed to be spherical. As shown in Fig. 3(a) and (d), the HAp powder surface had a dimple morphology when PVP was added. Also, the porous structure observed in the HAp powders adding PSB or PEG (Fig. 3(b,e), (c,f)). The bead-shaped spherical open pores were observed in the HAp powder to which PSB was added. Whereas the HAp powder adding PEG had skeletal structure.

In the USP process, it is divided into a first heating zone where D.I water is as a solvent evaporated and second heating zone where particles are synthesized. The first heating zone was set 200°C, and the second heating zone was set at 800°C. The decomposition temperature of the polymer was 450°C, 360°C, and <400°C in the order of the PVP, PSB, and PEG, which was lower than that of the HAp powder synthesized temperature (800°C). PVP is homogeneously dissolved in the HAp solution, and the polar chain of the PVP is grafted on the surface of the HAp. The polar chain of the PVP is caused by the coordinating bone between Ca^{2+} on the HAp surface and the oxygen atom of the carboxyl group [23]. It was assumed that the PVP was grafted not only to the surface of the particles but also to the inside of the particles as it was dissolved. The hydrophobic PSB was decomposed on the solid state to generate spherical pores in the form of the beads. PEG is hydrophilic such as the PVP and was soluble in the HAp solution, and the skeleton structure was observed as it was decomposed into a liquid state. Additionally, the decomposition of the HAp through oxidation of a carbon randomly placed between HAp aggregates was performed by the pyrolysis of PEG [24].

The additional heat treatment was conducted to remove the residue originated in the rapid synthesis rate on the USP process. Since the decomposition temperature of the polymer was lower than the heat treatment temperature of 600°C, it was expected that all residual polymers would be removed. In the case of the PVP added HAp, the dimple sizes by the image analysis were 179 ± 60 nm and 171 ± 35 nm for the USPed HAp powder and additional heat-treated HAp powder, respectively. Also, the pore sizes of the HAp synthesized adding PSB and PEG USPed HAp powders were 82 ± 15 nm and 293 ± 81 nm. The heat-treated HAp powder pore size was analyzed to be 78 ± 9 nm and 339 ± 99 nm for PSB and PEG, respectively. The pore sizes of PSB and PEG were similar to the USPed HAp powder and additional annealed HAp powder.

Fig. 4 is a specific surface area result by BET analysis. This is a graph showing the specific surface area results of raw USPed HAp powder, raw additional heat-treated HAp powder, and additional heat-treated HAp powder with each polymer added. The specific surface area of the raw USPed HAp powder and additional heat-treated HAp powder were 3.806 m^2/g and 14.581 m^2/g. And the HAp powders specific surface area by adding PVP, PSB, and PEG were additional heat-treated HAp powders 33.825 m^2/g, 16.732 m^2/g, and 21.345 m^2/g, respectively. The hollow structure of the HAp powder adding PVP could not be accurately observed, unlike the HAp powder with the PEG. It was suggested that the specific surface area of the HAp powder

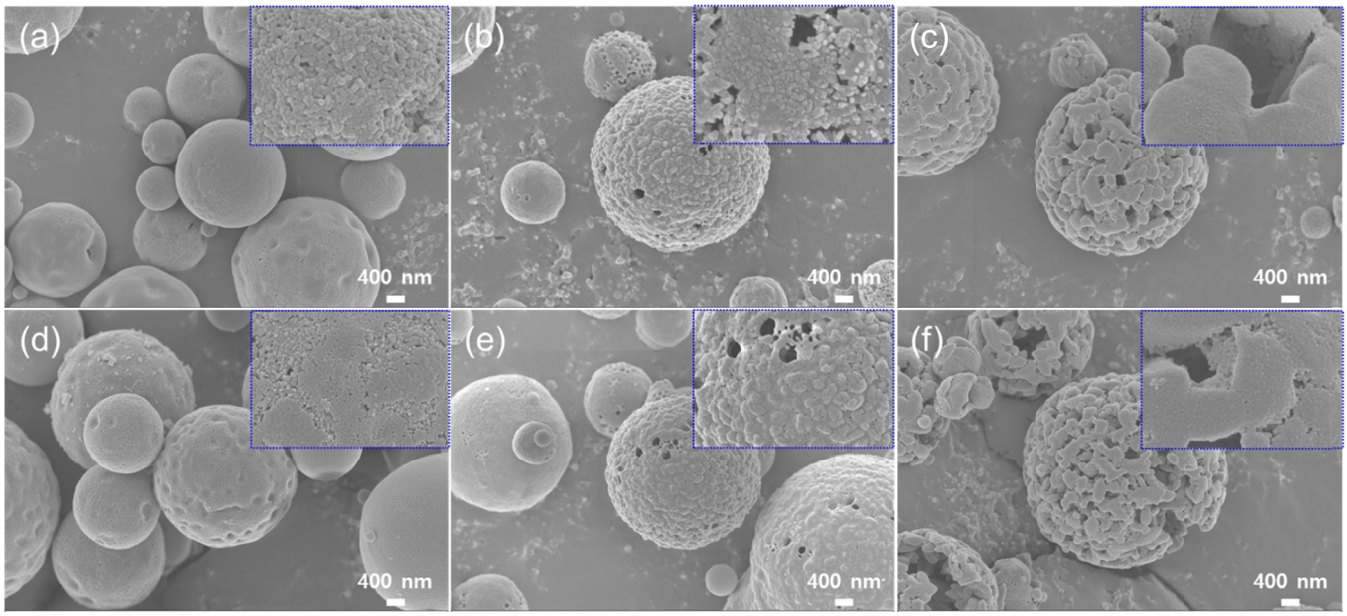

Fig. 3. FE-SEM images of the HAp synthesis adding (a, d) PVP (b, e) PSB and (c, f) PEG via (a-c) USP process and (d-f) additional heat treatment at 600°C for 2 h

with the PVP is higher due to the influence of the large amount the mesoporous. Hydrophobic PSB dissolves heterogeneously in the HAp solution. Therefore, since the porous structure does not appear, the specific surface area was the smallest value.

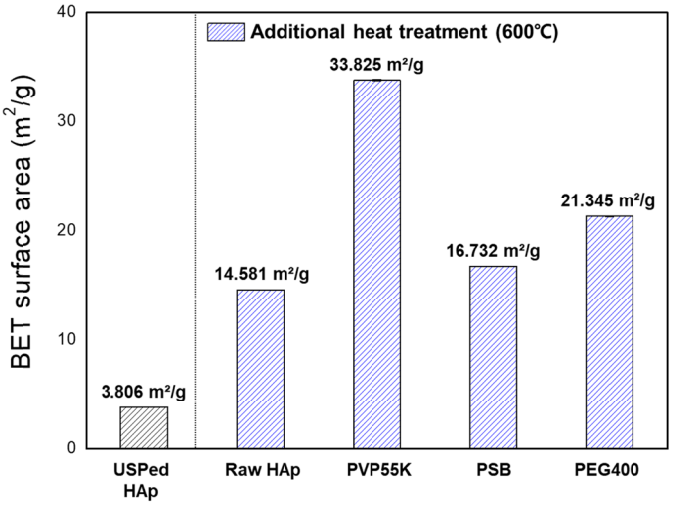

Fig. 4. BET analysis for all samples via USP process and additional heat treatment

4. Conclusions

The specific surface area was controlled by the property conditions of the polymer through the ultrasonic spray pyrolysis process. The polymers were used the PVP and PEG polymers of the hydrophilic property, and hydrophobic PSB. The powder prepared by adding the polymer also had a HAp single phase, and pores could be formed without any phase change. The powder prepared by adding PVP had a high specific surface area with a mesoporous dimple structure. HAp powder having a skeletal structure was synthesized because the PEG polymer dissolves hydrophilically in a liquid state. Finally, hydrophobic PSB was non-uniformly dissolved in the HAP solution and had the least effect on the specific surface area increase. In conclusion, it was confirmed that the particle characteristics such as the pore shape and specific surface area of the prepared HAp powder were controlled by the physical properties of the polymer.

Acknowledgments

The present research was supported by the research fund of Dankook University in 2022.

REFERENCES

[1] V. Uskoković, D.P. Uskoković, J. Biomed. Mater. Res. B Appl. Biomater. **96** (1), 152-191 (2011).
[2] H. Wang, Y. Li, Y. Zuo, J. Li, S. Ma, L. Cheng, Biomaterials **28** (22), 3338-3348 (2007).
[3] M. Aizawa, T. Hanazawa, K. Itatani, F.S. Howell, A. Kishioka, Mater. Sci. **34** (12), 2865-2873 (1999).
[4] T.M. Gabriel Chu, David G. Orton, Scott J. Hollister, Stephen E. Feinberg, John W. Halloran, Biomaterials **23** (5), 1283-1293 (2002).
[5] Karin A. Hing, Serena M. Best, K. Elizabeth Tanner, William Bonfield, Peter A. Revell, J. Biomed. Mater. Res. Part A. **68** (1), 187-200 (2004).
[6] J. Reichert, J.G.P. Binner, J. Mater. Sci. **31** (5), 1231-1241 (1996).
[7] A. Nayak, B. Bhushan, Mater. Today: Proc. **46**, 11029-11034 (2021).
[8] R. Stefini, G. Esposito, B. Zanotti, C. Iaccarino, M.M. Fontanella, F. Servadei, Surg. Neurol. Int. **4** (2013).
[9] L. Yang, X. Ning, K. Chen, H. Zhou, Ceram. Int. **33** (3), 483-489 (2007).
[10] M. Su, D.C.W. Tsang, X. Ren, Q. Shi, J. Tnag, H. Zhang, L. Kong, G. Song, D. Chen, Environ. Pollut. **254**, 112891 (2019).
[11] J. Roh, M. Yang, K.J. Lee, J. Powder Mater. **29**(6), 485-491 (2022).
[12] S. Lee, J. Roh, M. Kim, J. Lee, K.J. Lee, J. Mater. Sci. **57** (38), 18000-18013 (2022).
[13] S.C. Tsai, Y.L. Song, C.S. Tsai, C.C. Yang, W.Y. Chiu, H.M. Lin, J. Mater. Sci. **39** (11), 3647-3657 (2004).
[14] A.A.G. Santiago, C.R.R. Almeida, R.L. Tranquilin, R.M. Nascimento, C.A. Paskocimas, E. Longo, F.V Motta, M.R.D. Bomio, Ceram. Int. **44** (4), 3775-3786 (2018).
[15] A. Nakaruk, C.C. Sorrell, J. Coat. Technol. Res. **7** (5), 665-676 (2010).
[16] W.H. Shu, K.S. Suslick, J. Am. Chem. Soc. **127** (34), 12007-12010 (2005).
[17] Z. Kou, C. Wang, Mater. Adv. **3** (12), 4839-4850. (2022).
[18] J. Chen, S.K. Spear, J.G. Huddleston, R.D. Rogers, Green Chem. **7** (2), 64-82 (2005).
[19] E. Thormann, A.C. Simonsen, P.L. Hansen, O.G. Mouritsen, J. Am. Chem. Soc. **24** (14), 7278-7284 (2008).
[20] H. Kim, Y. Choi, Y. Park, R.C. pawar, Y.H. Choa, C. Lee, Curr. Appl. Phys. **17** (4), 433-441 (2017).
[21] U. Holzwarth, N. Gibson, Nat. Nanotechnol. **6** (9), 534-534 (2011).
[22] G.A. Ilevbare, H. Liu, K.J. Edgar, L.S. Taylor, Cryst. Growth Des. **12** (6), 3133-3143 (2012).
[23] Z. Song, Z. Yin, Z. Yang, C. Li, Z. Yang, C. Ning, D. Zhou, R. Wang, Y. Xu, J. Qiu, Mater. Sci. Eng. C, **32** (5), 1032-1036 (2012)
[24] J.S. Cho, S.H. Rhee, J. Eur. Ceram. Soc. **33** (2), 233-241 (2013).